Journal of Organic and Pharmaceutical Chemistry

Original Research

OPEN ACCESS
Freely available online on
http://ophcj.nuph.edu.ua

UDC 547.678.3; 547.812; 547.752; 535.34; 544.174.2

I. V. Kurdiukova, V. V. Kurdyukov, A. V. Kulinich
Institute of Organic Chemistry of the National Academy of Sciences of Ukraine,
5 Akademika Kukharya St., 02094 Kyiv, Ukraine

The Synthesis and Spectral Properties of Merocyanine Dyes Based on 9*H*-Fluorene-2,7-Dicarbonitrile

Dedicated to the cherished memory of Academician Alexander A. Ishchenko, a brilliant mentor and lifelong friend

Abstract
Di-, tetra-, and hexamethine merocyanine dyes bearing donor heterocyclic end groups of different electron-donating abilities and the 9*H*-fluorene-2,7-dicarbonitrile moiety as the acceptor end group have been synthesized. Their UV/Vis absorption spectra have been studied in solvents of varying polarity, and their electronic nature and vertical transitions have been investigated via (TD)-DFT calculations. The results indicate that the electronic structure of these merocyanines approaches the neutral polyene limit, becoming increasingly polyene-like in low-polarity solvents and upon increasing the polymethine chain length, which indicates the weak electron-acceptor ability of the 9*H*-fluorene-2,7-dicarbonitrile moiety. Nevertheless, longer vinylogs, especially those containing the 4*H*-pyran donor end group, exhibit the inverse solvatochromic behavior, which is highly unusual for such weakly dipolar merocyanines. A possible explanation for this effect has been proposed although its rigorous verification would require higher-level quantum-chemical calculations with solvent effects taken into account.
Keywords: merocyanines; fluorene; electronic absorption spectra; solvatochromism; TD-DFT calculations

І. В. Курдюкова, В. В. Курдюков, А. В. Кулініч
Інститут органічної хімії Національної академії наук України,
вул. Академіка Кухаря, 5, м. Київ, 02094, Україна

Синтез і спектральні властивості мероціанінів на основі 9*H*-флуорен-2,7-дикарбонітрилу

Анотація
Синтезовано ди-, тетра- та гексаметинові мероціанінові барвники, що містять донорні гетероциклічні кінцеві групи з різною електронодонорністю та фрагмент 9*H*-флуорен-2,7-дикарбонітрилу як акцепторну кінцеву групу. Їхні електронні спектри поглинання досліджено в розчинниках різної полярності, а електронну природу та електронні переходи проаналізовано за допомогою (TD)-DFT розрахунків. Отримані результати демонструють, що електронна структура цих мероціанінів близька до структури неполярного полієну, стаючи ще більш полієноподібною в малополярних розчинниках та зі збільшенням довжини поліметинового ланцюга, що свідчить про слабку електроноакцепторність фрагмента 9*H*-флуорен-2,7-дикарбонітрилу. Водночас довші вінілоги, особливо ті, що містять 4*H*-піран як донорну кінцеву групу, виявляють обернену сольватохромію, що є вкрай нетиповим для таких малополярних мероціанінів. Запропоновано можливе пояснення цього ефекту, однак його пильна перевірка потребуватиме квантово-хімічних обчислень методами вищого рівня та з урахуванням впливу розчинника.
***Ключові слова*:** мероціаніни; флуорен; електронні спектри поглинання; сольватохромія; TD-DFT розрахунки

Citation: Kurdiukova, I. V.; Kurdyukov, V. V.; Kulinich, A. V. The Synthesis and Spectral Properties of Merocyanine Dyes Based on 9*H*-Fluorene-2,7-Dicarbonitrile. *Journal of Organic and Pharmaceutical Chemistry* **2025**, *23* (4), 22–32.
https://doi.org/10.24959/ophcj.25.350444
Received: *2 October 2025*; **Revised:** *15 November 2025*; **Accepted:** *23 November 2025*

Funding: The authors received no specific funding for this work.
Conflict of interests: The authors have no conflict of interests to declare.

ISSN 2308-8303 (Print) / 2518-1548 (Online)

■ Introduction

Merocyanine dyes, owing to their broad range of practically important properties, such as pronounced solvatochromism, the ability to undergo substantial changes in the dipole moment upon electronic excitation, and the capacity to sensitize various physicochemical and chemical transformations, are increasingly being used in optoelectronics, nonlinear optics, data recording and processing technologies, as well as in medicine and biology [1, 2].

Among these, a special class features merocyanine dyes bearing a fluorene unit with electron-withdrawing substituents (EWGs) as the acceptor end group [3]. It has previously been shown that dyes containing nitro-substituted fluorene moieties exhibit the multi-band absorption in the Vis-NIR range, featuring additional charge-transfer bands at longer wavelengths, which may hamper their potential applications [4]. Therefore, it was of interest to develop analogs incorporating other EWGs capable of the effective conjugation with the π-electron system of the fluorene core, in particular cyano groups.

A preliminary (TD)-DFT evaluation of the electronic structure and electronic transitions in 9*H*-fluorene-2,7-dicarbonitrile derivatives suggested that, for such merocyanines, the polymethine $S_1^{FC} \leftarrow S_0$ transition is more clearly separated from higher-lying electronic transitions compared with nitro-substituted fluorene dyes. Accordingly, to verify this theoretical prediction, we synthesized and studied a series of merocyanine dyes for the first time incorporating the 9*H*-fluorene-2,7-dicarbonitrile moiety as the acceptor end group.

■ Results and Discussion

Synthesis and Structural Characterization

New merocyanines were synthesized via the Knoevenagel condensation between 9*H*-fluorene-2,7-dicarbonitrile (**1**) and the corresponding heterocyclic aldehydes or hemicyanines, giving two vinylogous series of dyes bearing 1,3,3-trimethyl-2*H*-indole and 2,6-di-*tert*-butyl-4*H*-pyran moieties as the donor end groups. For derivatives containing the more electron-donating indole core, the reaction was carried out under conventional conditions using triethylamine in acetic anhydride. In contrast, for the 2,6-di-*tert*-butyl-4*H*-pyran systems, a stronger base (DBU) and the higher-boiling solvent *N*,*N*-dimethylacetamide (DMAA) were required to increase the reaction rate and improve the yields (**Scheme 1**).

In the ^{1}H NMR spectra of the fluorene-based merocyanines **2**–**4** and **8**–**10** (see the ESI), as is

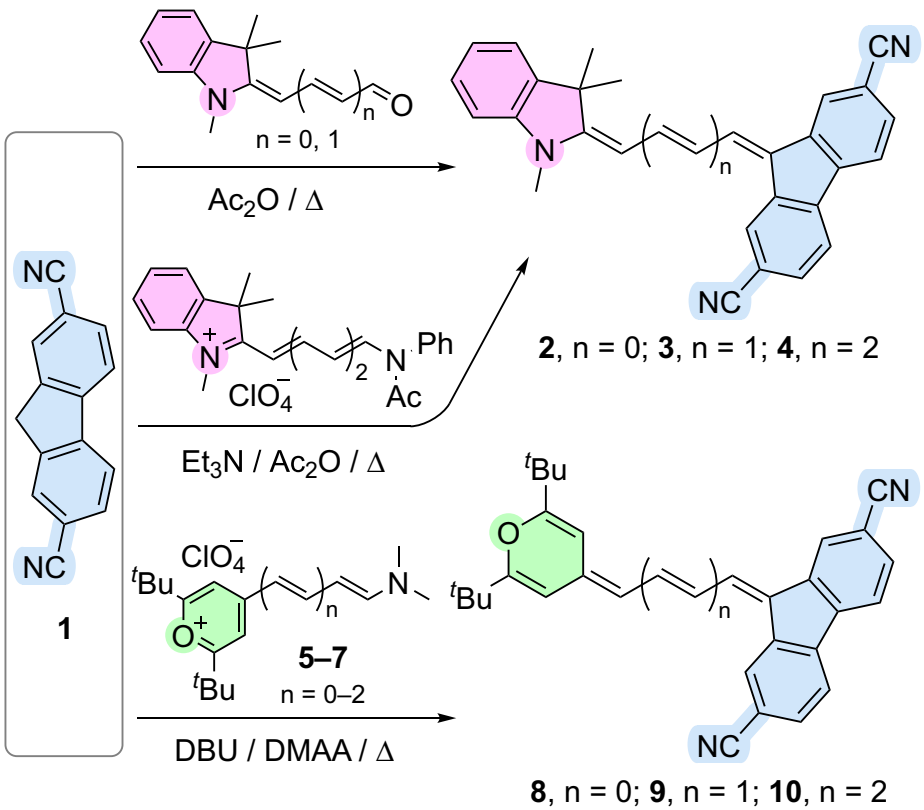

Scheme 1. The synthesis of novel fluorene-based merocyanines

generally the case for polymethines [2], an alternating pattern of chemical shifts is observed for the chain –CH= groups. This alternation reflects the corresponding alternation of the electron density along the polymethine chain. However, for these dyes, its value is lower than for more typical merocyanines. Thus, in compound **4**, the average chemical shift alternation for the polymethine chain protons H2, H3, and H4 is 0.71 ppm. (Counting starts from the donor heterocycle; these specific protons were selected as they were remote from the end groups, and thus not significantly affected by anisotropic end-group effects.) For similar indole-based hexamethines bearing malononitrile or thiobarbiturate acceptor groups, this alternation is equal to 1.00 and 1.11 ppm, respectively [5, 6] (all data recorded in $CDCl_3$).

For the pyran-based merocyanine **10**, the alternation is even smaller (0.55 ppm) and remains nearly unchanged (0.56 ppm) upon switching to highly polar $(CD_3)_2SO$. These data can be interpreted as evidence for a substantial contribution of the nonpolar polyene limiting structure to the electronic structure of the dyes synthesized [7].

This conclusion is further supported by the alternation of $^3J_{HH}$ spin–spin coupling constants in the polymethine chain, which amounts to 1.2 Hz for tetramethines **3** and **9** and increases to 2.2 Hz for hexamethine **10** [for compound **4**, the coupling constant between protons H4 and H5 could not be determined due to signal overlap and higher-order effects within the multiplet].

A decrease in the dipolar character of the merocyanines synthesized with chromophore lengthening is also evident in the series **2**–**4** from the decreasing chemical shift of the NMe group, which for vinylog **4** is 3.24 ppm (for comparison, the corresponding thiobarbituric-acid-acceptor analog exhibits a shift of 3.37 ppm [6]).

A decrease in the dipolar character of the merocyanines synthesized with chromophore lengthening is also evident in the series **2** – **3** – **4** from the decreasing chemical shift of the NMe group, which are 3.48, 3.35, and 3.24 ppm, respectively.

Solvatochromic Behavior

The solvents selected for the study of solvatochromism of the dyes synthesized included low-polarity cyclohexane (cHex; ε_D 2.02, n_D 1.427) and toluene (ε_D 2.37, n_D 1.496), medium-polarity dichloromethane (DCM; ε_D 8.9, n_D 1.424), and two polar non-protogenic solvents, acetonitrile (ε_D 36.2, n_D 1.344; electrophilic) and DMF (ε_D 36.7, n_D 1.430; nucleophilic) [8]. The corresponding spectral characteristics are summarized in **Table 1** (while the UV–Vis spectra of all dyes are provided in the ESI). The Bouguer–Lambert–Beer law is obeyed for merocyanines **2**–**4** and **8**–**10** over the concentration range of 1×10^{-6} to 3×10^{-5} M in all solvents studied, indicating that the recorded spectra arise from molecular (non-aggregated) species. Protogenic solvents (e.g., ethanol and methanol) were excluded from this study owing to the very low solubility of the dyes in these media.

Upon lengthening of the polymethine chain in the series **2**–**4**, broadening of the long-wavelength absorption band and a decrease in its intensity are observed (**Figure 1A**), along with a reduction in the vinylene shifts (**Table 1**). Even in the medium-polarity solvent DCM, the vinylene shifts for pairs **2** – **3** and **3** – **4** are only 42 and 39 nm, respectively. Taken together, these observations indicate, in accordance with the ^{1}H NMR data, that the ground-state electronic structure of merocyanines **2**–**4** is very close to that of a nonpolar polyene.

Table 1. Characteristics of the long-wavelength absorption bands of dyes **2**–**4** and **8**–**10** at 20 °C

Dye	Solvent	λ_{max} [nm]	$\varepsilon\times10^{-4}$ [$M^{-1}\times cm^{-1}$]
2	cHex	**498**; 470	**6.51**; 4.40
	PhMe	509	5.81
	DCM	512	5.77
	MeCN	510	5.53
	DMF	518	5.46
3	cHex	561; **530**	6.12; **7.40**
	PhMe	543	6.45
	DCM	554	6.65
	MeCN	552	6.55
	DMF	562	6.12
4	cHex	611; **580**; 549	3.06; **5.93**; 5.04
	PhMe	585	5.09
	DCM	593	4.98
	MeCN	580	4.89
	DMF	592	4.64
8	cHex	529; **498**; 472	2.69; **4.55**; 3.60
	PhMe	504	4.53
	DCM	512	4.60
	MeCN	508	4.52
	DMF	514	4.44
9	cHex	592; 554; **522**	2.27; 5.77; **6.02**
	PhMe	**556**; 534	**5.51**; 5.31
	DCM	551	5.37
	MeCN	538	5.55
	DMF	546	5.06
10	cHex	648; 598; **567**	1.23; 4.62; **6.17**
	PhMe	569	6.51
	DCM	579	6.27
	MeCN	559	6.34
	DMF	570	5.64

ISSN 2308-8303 (Print) / 2518-1548 (Online)

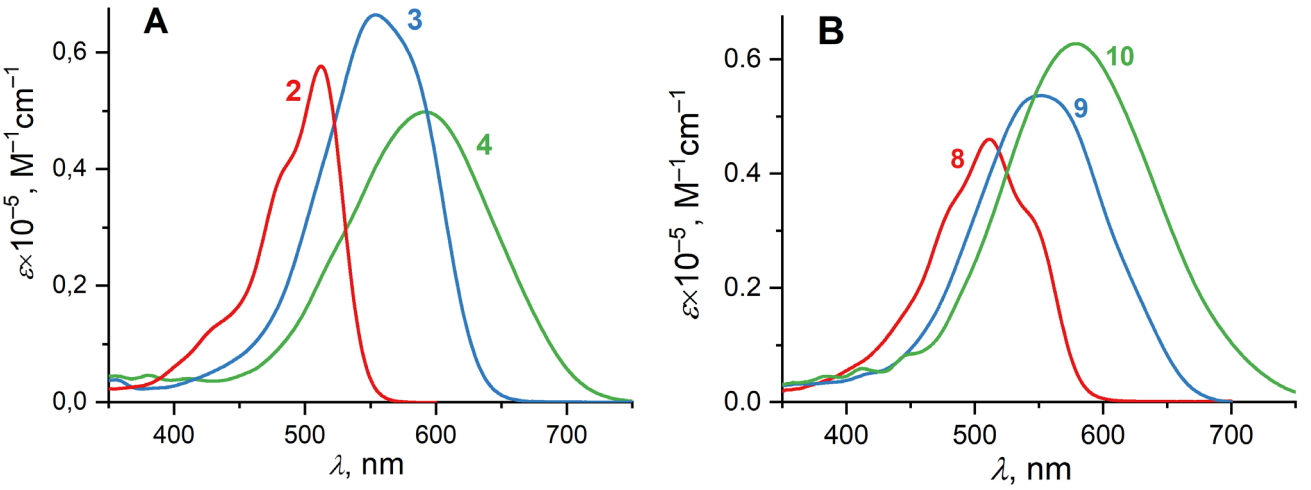

Figure 1. Electronic absorption spectra of dyes **2–4** (A) and **8–10** (B) in dichloromethane

For merocyanines **8–10**, increasing the chromophore length likewise leads to broadening and smoothing of the long-wavelength absorption band (**Figure 1B**). The vinylene shifts in DCM for pairs **8** – **9** and **9** – **10** are even smaller than those observed for the indole-based analogs **2–4**, amounting to 39 and 28 nm, respectively. These values are significantly lower than the typical ~100 nm vinylene shifts characteristic of symmetric cationic and anionic polymethines [9]. Once again, the spectral data for dyes **8–10** indicate that their electronic structure more closely resembles that of typical polyenes.

This conclusion is confirmed by comparison of the absorption ranges of the series **2–4** and **8–10**. Although the 4*H*-pyran moiety as the end group of polymethine dyes has a much greater "effective length" than the indole moiety [10, 11], the absorption maxima of merocyanines **8–10** are matching or even blue-shifted relative to those of their analogs **2–4** (**Table 1**).

Solvatochromic studies of dyes **2–4** and **8–10** revealed low sensitivity to the solvent nature. The position and shape of their long-wavelength absorption bands vary only slightly and not always consistently with increasing polarity. This is evident when comparing their absorption in the medium-polarity DCM and highly polar DMF (**Figure 2**). The only notable exceptions are the spectra in the least polar solvent, cHex, which exhibit a significant hypsochromic shift and a more pronounced fine structure (**Figure 2**, ESI). This striking divergence from just slightly more polar toluene can be attributed to the toluene higher refractive index, inducing a bathochromic shift [12], and the stronger solvation of polymethine chromophores by aromatic solvents via the solute–solvent π–π interactions [13].

Although small and only weakly dependent on the polymethine chain length, the solvatochromism of merocyanines **2–4** is positive (**Table 1**, **Figure 2**A). This effect is most evident for the

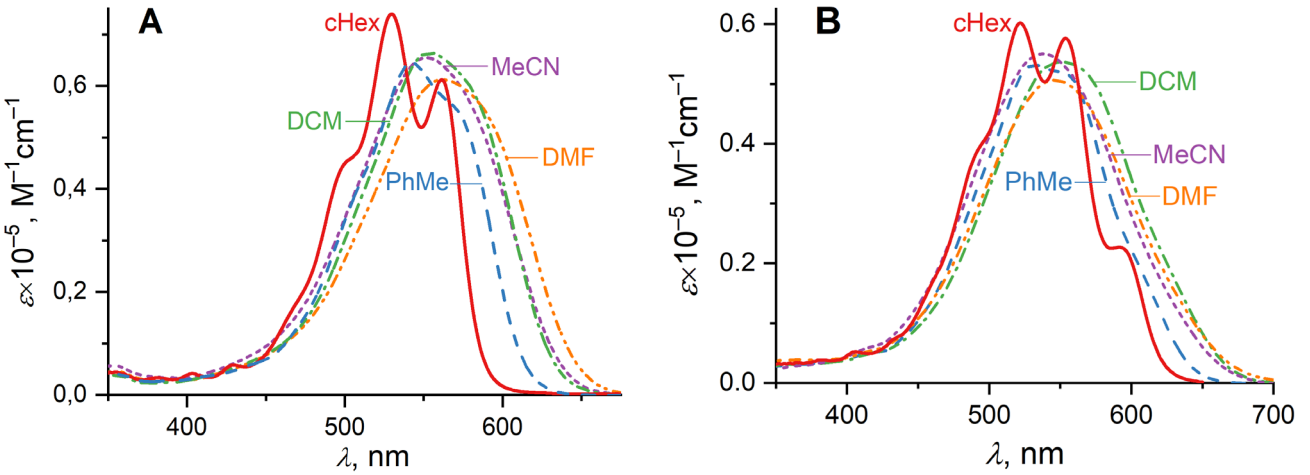

Figure 2. Electronic absorption spectra of dyes **3** (A) and **9** (B) in solvents of varying polarity

toluene–DCM and DCM–DMF solvent pairs, for which the refractive index changes only slightly or even decreases upon going to the more polar solvent [*this point is essential since the hypsochromic shifts observed upon going from DCM to MeCN can indeed be attributed to the decrease in the solvent refractive index* [12]]. In both cases, bathochromic shifts occur with increasing the solvent polarity, except for the longest vinylog **4**, for which the absorption maximum shifts 1 nm hypsochromically upon changing the solvent from DCM to DMF. Notably, the value of the solvatochromic effect, even when expressed on an energy scale (cm^{-1}), is maximal for tetramethine **3** and then decreases for hexamethine **4**. Such behavior may be considered indicative of an increasingly polyene-like nature of these chromophores with increasing the polymethine chain length, as is typical for merocyanines [2] since nonpolar polyenes are known to be insensitive to the solvent polarity, with their solvatochromism being governed entirely by the solvent polarizability [14].

A more intricate solvatochromic behavior is observed for the pyran-based dyes **8–10** (**Table 1**, **Figure 2**B). These compounds exhibit positive a solvatochromism in the toluene–DCM solvent pair, whereas in the DCM–DMF pair the changes in λ_{max} vary from +2 to –6 and then to –9 nm with increasing the polymethine chain length (**Table 1**). Even larger hypsochromic shifts are observed upon changing the solvent from DCM to MeCN; considering their value, these shifts cannot, as in the case of dyes **2–4**, be attributed solely to the lower refractive index of acetonitrile. Taken together, these observations point to the inverse solvatochromism for merocyanines **8–10**, at least for the longer vinylogs.

This result is highly unusual, given that (i) the pyran moiety is a weaker electron-donating end group than indole, and the indole-based analogs **2–4** exhibit a positive solvatochromism; (ii) trends in band shapes, and vinylene shifts indicate a polyene-like electronic structure for both merocyanine series; and (iii) higher vinylogs, due to their decreased dipolarity, typically tend toward a positive solvatochromism even when shorter vinylogs display the inverse behavior [2] rather than the opposite trend observed here.

DFT and TD-DFT Calculations

For all merocyanines **2–4** and **8–10**, the values of the $^3J_{HH}$ spin–spin coupling constants in the polymethine chain indicate the all-*trans* geometry, which is typical for polymethines. Accordingly, this geometry was chosen as the initial guess for the geometry optimization, performed in the vacuum approximation at the DFT-B3LYP/6-31G(d,p) level of theory and followed by frequency calculations to confirm that the located stationary points corresponded to true minima. The same functional and basis set were employed in the TD-DFT calculations of electronic transitions.

Although no symmetry constraints were imposed, the optimized ground-state geometries of the longer vinylogs **3**, **4**, **9**, and **10** were found to be essentially planar, with only negligible deviation from C_S-symmetry (the optimized atomic coordinates are provided in the ESI). Molecules **2** and **7** are more distorted, but even in these cases the interplanar angle between the end groups does not exceed 4.5°.

The proximity of the electronic structure of a merocyanine dye to one of the ideal limiting structures – nonpolar polyene, ideal polymethine or dipolar polyene – can be estimated from the degree of the bond-length (bond-order) alternation in its chromophore [15]. Usually, the bond-length alternation (BLA) and bond-order alternation (BOA) parameters are calculated as the difference between the averaged lengths or orders of formally single and formally double bonds in the "open" part of the polymethine chain (for merocyanines, the formal bond orders correspond to those in the nonpolar polyene limiting structure [7]). The BLA parameter takes positive values for structures in the nonpolar polyene–ideal polymethine range and negative values for those in the ideal polymethine–zwitterionic polyene range [15]; BOA has the opposite sign to BLA.

In the ground state S_0, the bond-length alternation in merocyanines **2–4** and **8–10** lies well within the positive range (**Table 2**), indicating a significant contribution from the nonpolar polyene limiting structure. This observation is in good agreement with the conclusions drawn from experimental ^{1}H NMR and UV–Vis spectral data. The BLA values increase with increasing the polymethine chain length, again correlating with the experimental results and well-established trends for such systems. However, a decrease in BLA is observed when going from indole- to 4*H*-pyran-based derivatives (**Table 2**), which is not consistent with the other results. At present, we do not have a satisfactory explanation for this behavior although it may indicate a case where long-range-corrected functionals, such as CAM-B3LYP or ωB97X, would be more appropriate.

According to the TD-DFT calculations, for all six molecules studied, the longest-wavelength

ISSN 2308-8303 (Print) / 2518-1548 (Online)

Table 2. Some results of the (TD-)DFT-B3LYP/6-31G(d,p) calculations for molecules **2**–**4** and **8**–**10**

Dye	BLA [Å]	$\mu(S_0)$ [Debye]	$\mu(S_1^{FC})$ [Debye]	$\mu(S_2^{FC})$ [Debye]	$S_1^{FC}\leftarrow S_0$		$S_2^{FC}\leftarrow S_0$	
					ΔE [eV]	f	ΔE [eV]	f
2	0.047	5.3	12.3	11.2	2.77	0.599	3.14	0.487
3	0.049	7.3	14.4	17.4	2.56	1.239	2.94	0.372
4	0.050	9.0	16.8	23.1	2.36	1.794	2.81	0.285
8	0.035	6.9	11.6	11.5	2.75	0.809	3.08	0.507
9	0.040	8.9	13.7	17.7	2.52	1.467	2.89	0.400
10	0.043	10.6	16.0	23.4	2.32	2.030	2.76	0.320

electronic transition is an allowed polymethine-type $^1\pi\pi^*$ transition, dominated by the HOMO→LUMO excitation, whose contribution ranges from 80 to 96% and increases for higher vinylogs. The calculated energies of the $S_1^{FC}\leftarrow S_0$ transition (**Table 2**) are in all cases somewhat higher than those estimated from the long-wavelength absorption maxima, which is in good agreement with literature data on the performance of TD-DFT for polymethine systems [16, 17]. This excitation is separated from the $S_2^{FC}\leftarrow S_0$ transition by an energy gap of 0.33–0.45 eV. The gap increases with the polymethine chain length (**Table 2**), yet remains comparatively narrow relative to that typically observed for polymethine dyes. Such a small separation can lead to a strong vibronic coupling and mixing of the two excited states. Indeed, the analysis of the contributing orbital transitions shows that the second-largest contribution to the $S_1^{FC}\leftarrow S_0$ transition arises from the HOMO→LUMO+1 excitation. Conversely, the HOMO→LUMO and HOMO→LUMO+1 contributions are interchanged in the $S_2^{FC}\leftarrow S_0$ transition. This state mixing is reflected as well in the relatively high oscillator strengths of the latter (0.28–0.51).

Comparative TD-DFT calculations for molecules **4** and **10** performed with the long-range-corrected CAM-B3LYP functional (using B3LYP-optimized molecular geometries) yielded results differing markedly from those obtained with B3LYP. Within this approximation, the energy gap between the S_1^{FC} and S_2^{FC} states is about 1 eV, significantly larger than in the B3LYP calculations, and the HOMO→LUMO excitation provides the dominant contribution (>95%) to the long-wavelength transition. A reduction in vibronic coupling between these states is reflected in the oscillator strengths for the $S_1^{FC}\leftarrow S_0$ transition that are 5–7 times smaller than those obtained with B3LYP. Overall, these calculations show substantially poorer agreement with the experimental observations than the B3LYP results.

Hence, despite preliminary TD-DFT evaluations suggesting that in 9*H*-fluorene-2,7-dicarbonitrile-based merocyanines the polymethine $S_1^{FC}\leftarrow S_0$ transition is more strongly separated from higher-lying electronic transitions than in (polynitro)fluorene-based analogs, this gap remains sufficiently small to allow their interaction, thereby influencing the photophysical properties of the new dyes. We therefore reckon that the absence of detectable fluorescence for dyes **2**–**4** and **8**–**10** can be attributed to this effect, which leads to a stronger vibronic coupling and, consequently, an enhanced excited-state deactivation via the internal conversion. Notably, the presence of a higher-lying electronic transition can be discerned at first glance only from the band shapes of dye **2** (**Figure 1A**). In the other cases, the absorption bands are too broad and diffuse to allow its direct identification. Nevertheless, based on the above data, it must be assumed that for all dyes studied the long-wavelength absorption band corresponds not to a single but to two electronic transitions. Such a situation, which is unusual for polymethine dyes, may be responsible for the atypical solvatochromism observed for these compounds.

The analysis of the topography of the molecular orbitals involved (**Figure 3**), as well as of the electron-density redistribution associated with the discussed transitions (**Figure 4**), reveals that the $S_1^{FC}\leftarrow S_0$ transition is predominantly of the polymethine type. However, the HOMO and LUMO exhibit an increased localization on the donor and acceptor end groups, respectively, which imparts a partial charge-transfer character to this excitation. Accordingly, it is accompanied by the donor-to-acceptor electron-density redistribution, manifested as an increase in the molecular dipole moment (**Table 2**).

In contrast, the LUMO+1 exhibits a substantially stronger localization than the LUMO on the 9*H*-fluorene-2,7-dicarbonitrile moiety (**Figure 3**), implying that the $S_2^{FC}\leftarrow S_0$ transition should possess a more pronounced charge-transfer

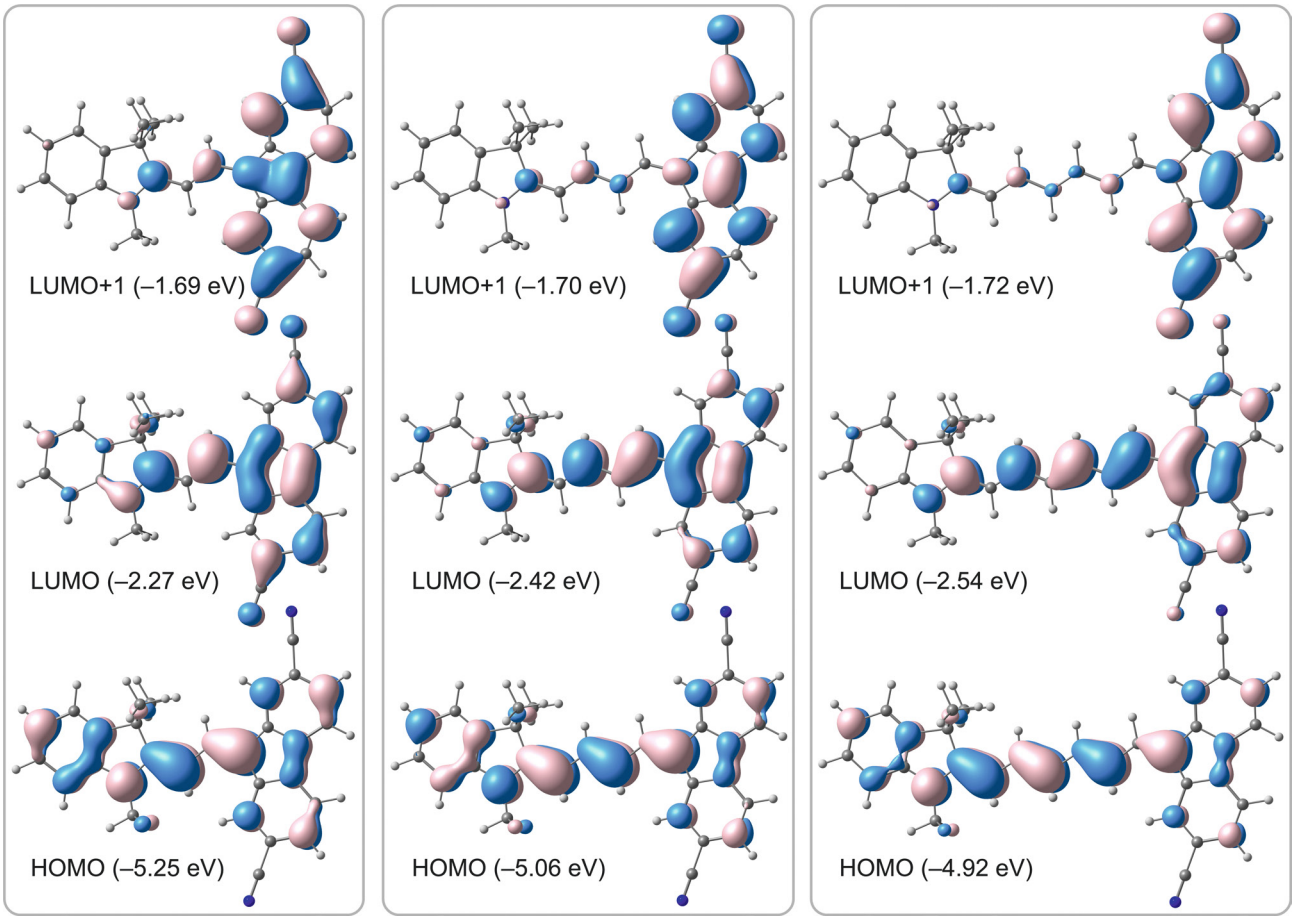

Figure 3. Molecular orbitals of dyes **2**–**4** (DFT-B3LYP/6-31G(d,p); the contour value is 0.03 bohr$^{-3/2}$)

nature (**Figure 4**) and give rise to a more dipolar excited state. Nevertheless, for dimethines **2** and **9**, for which the short polymethine chain length results in very similar spatial localizations of the LUMO and LUMO+1 (**Figure 3**), the increase in the dipole moment upon the $S_2^{FC}\leftarrow S_0$ excitation is smaller than that associated with the $S_1^{FC}\leftarrow S_0$ transition (**Table 2**).

We assume that the more dipolar nature of the S_2^{FC} state, at least in the higher vinylogs of the dyes studied, may be responsible for their atypical solvatochromism. Its preferential stabilization relative to the S_1^{FC} state in high-polarity solvents can lead to further enhancement of the vibronic coupling between these two states and to an increase in the oscillator strength of the $S_2^{FC}\leftarrow S_0$ transition. In the case of broad and diffuse long-wavelength absorption bands, this would shift the band maximum hypsochromically in agreement with the experimental observations.

However, verification of this assumption would require both the solvent modelling and the application of higher-level electronic-structure methods, such as ADC(2), to reliably describe the strongly coupled excited states. An argument against relying on TD-DFT for this purpose is the appearance of pronounced de-excitation contributions in the TD-DFT description of the lowest electronic transition for merocyanines **4**, **9**, and **10** (precisely those exhibiting inverse solvatochromism), which

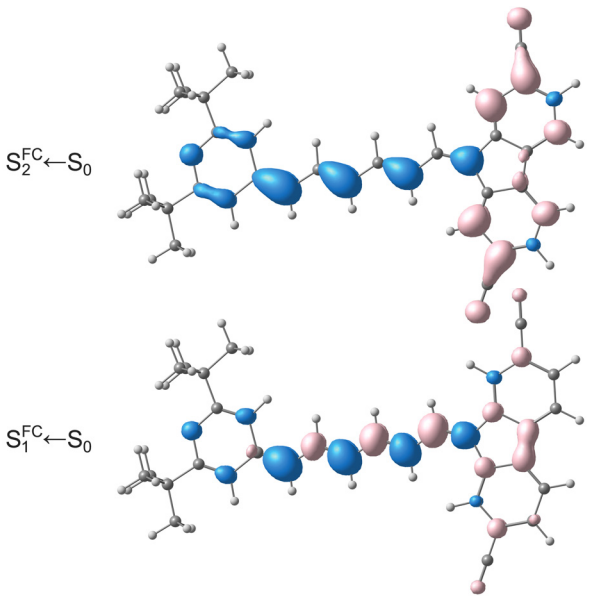

Figure 4. Electron density changes upon excitations in molecule **10** (increase in light-red, decrease in blue; the contour value is 0.002 e×bohr^{-3})

ISSN 2308-8303 (Print) / 2518-1548 (Online)

suggests a substantial ground–excited-state mixing [18]. In such cases, even small solvent-induced perturbations may alter the balance between excitation and de-excitation contributions, potentially giving rise to the anomalous solvatochromic behavior.

■ Conclusions

A series of di-, tetra-, and hexamethine merocyanine dyes incorporating heterocyclic donor end groups and the 9*H*-fluorene-2,7-dicarbonitrile acceptor moiety has been synthesized and comprehensively characterized by the UV–Vis spectroscopy and (TD)-DFT calculations. The combined experimental and computational analysis demonstrates that the electronic structure of these dyes lies close to the neutral polyene limit (the polyene-like character becomes more pronounced with increasing polymethine chain length) suggesting the relatively weak electron-acceptor character of the 9*H*-fluorene-2,7-dicarbonitrile fragment.

Surprisingly, despite their overall weak dipolar character, the longer vinylogs, particularly those bearing the 4*H*-pyran donor end group, exhibit a pronounced inverse solvatochromism. TD-DFT calculations suggest that this unusual behavior may be associated with a small energy separation between the two lowest $^1\pi\pi^*$ excited states, resulting in a strong vibronic coupling and state mixing. The higher-lying excited state possesses a more pronounced charge-transfer character and, for the higher vinylogs, a larger dipole moment, making it especially sensitive to the solvent polarity. Preferential stabilization of this state in polar media may enhance its contribution to the long-wavelength absorption band, leading to its hypsochromic shift despite the weak ground-state dipolarity of the dyes.

The absence of detectable fluorescence for all these merocyanines is likewise attributed, in addition to their polyene-like electronic structure, to efficient nonradiative deactivation pathways promoted by a strong vibronic coupling between closely spaced excited states. The presence of significant de-excitation contributions in the TD-DFT description of the lowest electronic transition for dyes exhibiting the inverse solvatochromism further suggests a substantial ground–excited-state mixing, underscoring the limitations of TD-DFT for the quantitative description of such systems.

Overall, this study has revealed an unconventional mechanism that can influence the solvatochromic behavior even of weakly dipolar donor–acceptor systems when their excited-state manifold is strongly coupled and sensitive to solvent-induced perturbations. For the final verification of the mechanism proposed, higher-level excited-state methods combined with solvent modelling will be required.

■ Experimental Part

Solvents for spectral measurements were purified according to standard procedures [19]. ^{1}H NMR spectra were recorded on Varian VXR (300 MHz) and Varian Unity (400 MHz) spectrometers. The residual solvent peaks were used as internal standards: $CDCl_3$, δ_H = 7.27 ppm; $(CD_3)_2SO$, δ_H = 2.50 ppm. Electronic absorption spectra were recorded at 20 °C using a Shimadzu UV-3100 spectrophotometer and 1-cm quartz cuvettes. Analytical TLC was performed on Silufol UV-254 silica gel plates. Purification of dyes was carried out by column chromatography using Silica gel (70–230 μm, Merck) or Aluminum oxide 90 (63–200 μm, Merck). Melting (decomposition) points were determined in open capillaries and are reported without correction. DFT and TD-DFT calculations were performed with the Gaussian-09 program suite [20] using the B3LYP hybrid functional [21] and the double-ζ basis set 6-31G(d,p).

9-[2-(1,3,3-Trimethylindol-2-ylidene)ethylidene]-9*H*-fluorene-2,7-dicarbonitrile (2)

A mixture of 9*H*-fluorene-2,7-dicarbonitrile **1** [22] (108 mg, 0.5 mmol) and 2-(1,3,3-trimethylindol-2-ylidene)acetaldehyde (101 mg, 0.5 mmol) in acetic anhydride (1.5 mL) was heated until complete dissolution of the reagents was achieved. The resulting solution was then refluxed for an additional 3 min, during which time it turned deep red. After cooling to room temperature, the precipitate was filtered off and washed successively with acetic acid and water. The crude product was purified by column chromatography on silica gel using chloroform as an eluent.

A red solid. Yield 60 mg (30%). M. p. 243–245 °C. Anal. Calcd for $C_{28}H_{21}N_3$, %: C 84.18; H 5.30; N 10.52. Found, %: C 83.97; H 5.24; N 10.39. ^{1}H NMR (300 MHz, $CDCl_3$), *δ,* ppm: 1.82 (6H, s, $C(CH_3)_2$), 3.48 (3H, s, NCH_3), 6.31 (1H, d, *J* = 13.5 Hz, –CH=), 6.91 (1H, d, *J* = 8.0 Hz), 7.08 (1H, t, *J* = 7.5 Hz), 7.29–7.36 (2H, m), 7.57 (1H, dd, *J* = 8.0, 1.3 Hz), 7.64 (1H, dd, *J* = 8.0, 1.3 Hz), 7.94 (1H, d, *J* = 8.0 Hz), 8.01 (1H, d, *J* = 8.1 Hz), 8.03 (1H, s), 8.09 (1H, d, *J* = 13.5 Hz, –CH=), 8.27 (1H, s).

9-[4-(1,3,3-Trimethylindol-2-ylidene)-2-buten-1-ylidene]-9*H*-fluorene-2,7-dicarbonitrile (3)

The compound was synthesized similarly to **2**, starting from 4-(1,3,3-trimethylindol-2-ylidene)-2-butenal. The crude product was purified by column chromatography on silica gel using DCM as an eluent and then crystallized from acetonitrile.

A khaki with a metal shine solid. Yield 120 mg (56%). M. p. > 280 °C. Anal. Calcd for $C_{30}H_{23}N_3$, %: C 84.68; H 5.45; N 9.87. Found, %: C 84.45; H 5.40; N 9.78. ^{1}H NMR (300 MHz, $CDCl_3$), δ, ppm: 1.71 (6H, s, $C(CH_3)_2$), 3.35 (3H, s, NCH_3), 5.81 (1H, d, J = 12.4 Hz, –CH=), 6.79 (1H, d, J = 7.9 Hz), 6.99 (1H, t, J = 7.5 Hz), 7.06 (1H, t, J = 13.0 Hz, –CH=), 7.22–7.30 (2H, m), 7.50 (1H, t, J = 13.0 Hz, –CH=), 7.54 (1H, d, J = 12.5 Hz, –CH=), 7.57 (1H, dd, J = 8.0, 1.3 Hz), 7.63 (1H, dd, J = 7.9, 1.3 Hz), 7.89 (1H, d, J = 7.9 Hz), 7.94 (1H, d, J = 8.0 Hz), 8.08 (1H, s), 8.38 (1H, s).

9-[6-(1,3,3-Trimethylindol-2-ylidene)-2,4-hexadien-1-ylidene]-9*H*-fluorene-2,7-dicarbonitrile (4)

A mixture of **1** (108 mg, 0.5 mmol) and 2-[6-(acetylphenylamino)-1,3,5-hexatrien-1-yl]-1,3,3-trimethyl-3*H*-indolium perchlorate (236 mg, 0.5 mmol) in acetic anhydride (2 mL) was heated until complete dissolution of the reagents. Then triethylamine (150 mg, 1.5 mmol) was added, and the reaction mixture was refluxed for additional 15 min. After cooling, it was poured into a saturated $NaHCO_3$ solution (100 mL) and left for 12 h. The solid precipitate was filtered off, washed with water, dried, and then purified by column chromatography on Al_2O_3 using DCM as an eluent.

A brown-bronze solid. Yield 50 mg (11%). M. p. 235–236 °C. Anal. Calcd for $C_{32}H_{25}N_3$, %: C 85.11; H 5.58; N 9.31. Found, %: C 84.93; H 5.55; N 9.19. ^{1}H NMR (300 MHz, $CDCl_3$), δ, ppm: 1.66 (6H, s, $C(CH_3)_2$), 3.24 (3H, s, NCH_3), 5.56 (1H, d, J = 12.3 Hz, –CH=), 6.42 (1H, dd, J = 13.8, 10.4 Hz, –CH=), 6.72 (1H, d, J = 7.9 Hz), 6.94 (1H, t, J = 7.5 Hz), 7.04 (1H, t, J = 12.7 Hz, –CH=), 6.98–7.17 (2H, m, 2 –CH=), 7.17–7.29(3H, m, 2ArH + –CH=), 7.43 (1H, d, J = 11.3 Hz, –CH=), 7.59 (1H, dd, J = 8.0, 1.3 Hz), 7.64 (1H, dd, J = 8.1, 1.3 Hz), 7.87 (1H, d, J = 8.0 Hz), 7.92 (1H, d, J = 8.1 Hz), 8.00 (1H, s), 8.30 (1H, s).

Hemicyanines 5 and 6 were prepared according to the ref [23].

2,6-Di-*tert*-butyl-4-[6-(dimethylamino)-1,3,5-hexatrien-1-yl]pyrylium perchlorate (7)

(i) A mixture of 2,6-di-*tert*-butyl-4-methylpyrylium perchlorate (1.53 g, 5.0 mmol) and *N*-[5-(phenylimino)-1,3-pentadienyl]aniline hydrochloride (1.43 g, 5.0 mmol) in a mixture of acetic anhydride and acetic acid (2:1, *v*/*v*; 10 mL) was refluxed for 10 min, then cooled to room temperature. The resulting intermediate hemicyanine was precipitated by the addition of an aqueous sodium perchlorate solution, filtered off, and dried. The crude product was used in the subsequent step without further purification.

(ii) The material thus obtained was dissolved in acetonitrile (5 mL), after which a 25% ethanol solution of dimethylamine (2 mL) was added. The reaction mixture was stirred for 30 min at 20 °C. Hemicyanine **7** was precipitated by the addition of an aqueous sodium perchlorate solution, filtered off, washed with water, and dried. The final purification was achieved by column chromatography on silica gel using chloroform–ethanol (98:2, *v*/*v*) as an eluent, followed by crystallization from an acetonitrile–diethyl ether mixture.

Blue-violet bladed crystals. Yield 0.58 g (28%). M. p. 174–175 °C. Anal. Calcd for $C_{21}H_{32}ClNO_5$, %: C 60.93; H 7.79; Cl 8.56; N 3.38. Found, %: C 60.77; H 7.75; Cl 8.59; N 3.40. ^{1}H NMR (400 MHz, $CDCl_3$), δ, ppm: 1.27 (9H, s, $C(CH_3)_3$), 1.32 (9H, s, $C(CH_3)_3$), 3.24 (3H, s, NCH_3), 3.51 (3H, s, NCH_3), 5.78 (1H, d, J = 12.9 Hz, –CH=), 5.98 (1H, t, J = 12.3 Hz, –CH=), 6.06 (1H, d, J = 1.8 Hz), 6.34 (1H, t, J = 12.8 Hz, –CH=), 6.63 (1H, d, J = 1.8 Hz), 7.66 (1H, t, J = 13.1 Hz, –CH=), 7.76 (1H, t, J = 12.8 Hz, –CH=), 8.12 (1H, d, J = 11.4 Hz, –CH=).

9-[2-(2,6-Di-*tert*-butyl-4*H*-pyran-4-ylidene)-ethylidene]-9*H*-fluorene-2,7-dicarbonitrile (8)

To the solution of hemicyanine **5** (180 mg, 0.5 mmol) in DMAA (2 mL), compound **1** (110 mg, 0.5 mmol) and DBU (80 mg, 0.53 mmol) were added. The mixture was heated at 160 °C for 2.5 h. After cooling to room temperature, the dye was precipitated with brine, filtered off, and washed with water. The crude product was purified by column chromatography using chloroform–ethyl acetate (98:2, *v*/*v*) as an eluent, followed by crystallization from acetonitrile.

A beetroot-red solid. Yield 76 mg (28%). M. p. > 280 °C. Anal. Calcd for $C_{30}H_{28}N_2O$, %: C 83.30; H 6.52; N 6.48. Found, %: C 83.11; H 6.50; N 6.40. ^{1}H NMR (400 MHz, $CDCl_3$), δ, ppm: 1.32 (9H, s, $C(CH_3)_3$), 1.37 (9H, s, $C(CH_3)_3$), 6.17 (1H, s), 6.47 (1H, d, J = 13.2 Hz, –CH=), 6.53 (1H, s), 7.57 (1H, d, J = 8.0 Hz), 7.63 (1H, d, J = 8.1 Hz), 7.79 (1H, d, J = 13.2 Hz, –CH=), 7.91 (1H, d, J = 8.0 Hz), 7.96 (1H, d, J = 8.1 Hz), 8.09 (1H, s), 8.37 (1H, s).

ISSN 2308-8303 (Print) / 2518-1548 (Online)

9-[4-(2,6-Di-*tert*-butyl-4*H*-pyran-4-ylidene)-2-buten-1-ylidene]-9*H*-fluorene-2,7-dicarbonitrile (9)

The compound was synthesized similarly to **8**, starting from hemicyanine **6**, purified by column chromatography using chloroform as an eluent, and then crystallized from acetonitrile.

Dark-green needles. Yield 62 mg (28%). M. p. > 280 °C. Anal. Calcd for $C_{32}H_{30}N_2O$, %: C 83.81; H 6.59; N 6.11. Found, %: C 83.59; H 6.50; N 6.00. ^{1}H NMR (400 MHz, $CDCl_3$), δ, ppm: 1.25 (9H, s, $C(CH_3)_3$), 1.30 (9H, s, $C(CH_3)_3$), 5.85 (1H, d, J = 12.3 Hz, −CH=), 5.86 (1H, s), 6.28 (1H, s), 7.07 (1H, t, J = 13.0 Hz, −CH=), 7.26 (1H, t, J = 12.9 Hz, −CH=), 7.51 (1H, d, J = 12.5 Hz, −CH=), 7.57 (1H, dd, J = 7.9, 1.3 Hz), 7.63 (1H, dd, J = 8.0, 1.3 Hz), 7.87 (1H, d, J = 7.9 Hz), 7.92 (1H, d, J = 8.0 Hz), 8.04 (1H, s), 8.30 (1H, s).

9-[6-(2,6-Di-*tert*-butyl-4*H*-pyran-4-ylidene)-2,4-hexadien-1-ylidene]-9*H*-fluorene-2,7-dicarbonitrile (10)

The compound was synthesized similarly to **8**, starting from hemicyanine **7**, at 120 °C for 1 h, and purified similarly to **9**.

Dark green with metal shine needles. Yield 77 mg (32%). M. p. 273–275 °C. Anal. Calcd for $C_{34}H_{32}N_2O$, %: C 84.26; H 6.67; N 5.78. Found, %: C 83.59; H 6.62; N 5.70. ^{1}H NMR (300 MHz, $CDCl_3$), δ, ppm: 1.22 (9H, s, $C(CH_3)_3$), 1.26 (9H, s, $C(CH_3)_3$), 5.63 (1H, d, J = 12.2 Hz, −CH=), 5.76 (1H, s), 6.15 (1H, s), 6.44 (1H, dd, J = 14.0, 11.2 Hz, −CH=), 6.92–7.05(2H, m, 2 −CH=), 7.13 (1H, t, J = 13.0 Hz, −CH=), 7.38 (1H, d, J = 12.2 Hz, −CH=), 7.59 (1H, d, J = 7.9 Hz), 7.64 (1H, d, J = 7.9 Hz), 7.86 (1H, d, J = 7.9 Hz), 7.91 (1H, d, J = 7.9 Hz), 7.98 (1H, s), 8.29 (1H, s). *The ^{1}H NMR chemical shifts of this dye in $CDCl_3$ were found to be concentration-dependent, likely due to aggregation. The values reported herein correspond to the solution of 4 mg of the dye in 0.67 mL of $CDCl_3$.* ^{1}H NMR (300 MHz, $(CD_3)_2SO$), δ, ppm: 1.18 (9H, s, $C(CH_3)_3$), 1.22 (9H, s, $C(CH_3)_3$), 5.66 (1H, d, J = 12.2 Hz, −CH=), 6.32 (1H, s), 5.89 (1H, s), 6.59 (1H, dd, J = 14.1, 11.5 Hz, −CH=), 7.09 (1H, dd, J = 13.9, 11.5 Hz, −CH=), 7.20 (1H, dd, J = 14.1, 12.2 Hz, −CH=), 7.52 (1H, dd, J = 13.9, 12.5 Hz, −CH=), 7.78 (1H, d, J = 8.0 Hz), 7.79 (1H, d, J = 12.5 Hz, −CH=), 7.85 (1H, d, J = 7.9 Hz), 8.21 (1H, d, J = 8.0 Hz), 8.27 (1H, d, J = 7.9 Hz), 8.48 (1H, s), 8.70 (1H, s).

Acknowledgement

The quantum-chemical calculations were performed using the computational facilities of the joint computational cluster of the State Scientific Institution “Institute for Single Crystals”, and the Institute for Scintillation Materials of NAS of Ukraine incorporated into the Ukrainian National Grid.

References

1. Mishra, A.; Behera, R. K.; Behera, P. K.; Mishra, B. K.; Behera, G. B. Cyanines during the 1990s: A Review. *Chem. Rev.* **2000,** *100* (6), 1973–2012. https://doi.org/10.1021/cr990402t.
2. Kulinich, A. V.; Ishchenko, A. A. Merocyanines: Electronic Structure and Spectroscopy in Solutions, Solid State, and Gas Phase. *Chem. Rev.* **2024,** *124* (21), 12086–12144. https://doi.org/10.1021/acs.chemrev.4c00317.
3. Kurdyukova, I. V.; Ishchenko, A. A. Organic dyes based on fluorene and its derivatives. *Russ. Chem. Rev.* **2012,** *81* (3), 258. https://doi.org/10.1070/RC2012v081n03ABEH004211.
4. Kurdyukova, I. V.; Ishchenko, A. A.; Derevyanko, N. A.; Mysyk, D. D. Synthesis and Spectral Properties of Merocyanine Dyes Derived from Tetranitrofluorene and Heterocycles of Various Electron-donating Ability. *Chem. Heterocycl. Comp.* **2013,** *49* (2), 281–293. https://doi.org/10.1007/s10593-013-1245-x.
5. Kulinich, A. V.; Ishchenko, A. A.; Groth, U. M. Electronic structure and solvatochromism of merocyanines: NMR spectroscopic point of view. *Spectrochim. Acta, Part A* **2007,** *68* (1), 6–14. https://doi.org/10.1016/j.saa.2006.10.043.
6. Kulinich, A. V.; Derevyanko, N. A.; Ishchenko, A. A. Electronic structure and solvatochromism of merocyanines based on N,N-diethylthiobarbituric acid. *J. Photoch. Photobio. A* **2007,** *188* (2), 207–217. https://doi.org/10.1016/j.jphotochem.2006.12.014.
7. Dähne, S. Der Ideale Polymethinzustand. *Chimia* **1991**, *45* (10), 288. https://doi.org/10.2533/chimia.1991.288.
8. Reichardt, C.; Welton, T. Solvents and solvent effects in organic chemistry: Fourth edition, Wiley-VCH, Weinheim, 2010. https://doi.org/10.1002/9783527632220.
9. König, W. Über den Begriff der „Polymethinfarbstoffe” und eine davon ableitbare allgemeine Farbstoff-Formel als Grundlage einer neuen Systematik der Farbenchemie. *Journal für Praktische Chemie* **1926,** *112* (1), 1–36. https://doi.org/10.1002/prac.19261120101.
10. Reynolds, G. A.; Drexhage, K. H. Stable heptamethine pyrylium dyes that absorb in the infrared. *J. Org. Chem.* **1977,** *42* (5), 885–888. https://doi.org/10.1021/jo00425a027.
11. Pascal, S.; Getmanenko, Y. A.; Zhang, Y.; Davydenko, I.; Ngo, M. H.; Pilet, G.; Redon, S.; Bretonnière, Y.; Maury, O.; Ledoux-Rak, I.; Barlow, S.; Marder, S. R.; Andraud, C. Design of Near-Infrared-Absorbing Unsymmetrical Polymethine Dyes with Large Quadratic Hyperpolarizabilities. *Chem. Mater.* **2018,** *30* (10), 3410–3418. https://doi.org/10.1021/acs.chemmater.8b00960.
12. Renge, I. Refractive index dependence of solvatochromism. *J. Photoch. Photobio. A* **2018,** *353*, 433–444. https://doi.org/10.1016/j.jphotochem.2017.11.048.
13. Ishchenko, A. A.; Svidro, V. A.; Derevyanko, N. A. Solvatofluorochromy of cationic cyanine dyes. *Dyes Pigments* **1989,** *10* (2), 85–96. https://doi.org/10.1016/0143-7208(89)85001-6.

14. Catalán, J. Toward a Generalized Treatment of the Solvent Effect Based on Four Empirical Scales: Dipolarity (SdP, a New Scale), Polarizability (SP), Acidity (SA), and Basicity (SB) of the Medium. *J. Phys. Chem. B* **2009,** *113* (17), 5951–5960. https://doi.org/10.1021/jp8095727.
15. Meyers, F.; Marder, S. R.; Pierce, B. M.; Bredas, J. L. Electric Field Modulated Nonlinear Optical Properties of Donor-Acceptor Polyenes: Sum-Over-States Investigation of the Relationship between Molecular Polarizabilities (.alpha., .beta., and .gamma.) and Bond Length Alternation. *J. Am. Chem. Soc.* **1994,** *116* (23), 10703–10714. https://doi.org/10.1021/ja00102a040.
16. Fabian, J. TDDFT-calculations of Vis/NIR absorbing compounds. *Dyes Pigments* **2010,** *84* (1), 36–53. https://doi.org/10.1016/j.dyepig.2009.06.008.
17. Tomar, R.; Bernasconi, L.; Fazzi, D.; Bredow, T. Theoretical Study on the Optoelectronic Properties of Merocyanine-Dyes. *J. Phys. Chem. A* **2023,** *127* (46), 9661–9671. https://doi.org/10.1021/acs.jpca.3c04226.
18. Plasser, F. On the Meaning of De-Excitations in Time-Dependent Density Functional Theory Computations. *J. Comput. Chem.* **2025,** *46* (8), e70072. https://doi.org/10.1002/jcc.70072.
19. Armarego, W. L. F.; Chai, C. Purification of Laboratory Chemicals, 6th ed., Butterworth-Heinemann, Oxford, 2009. https://doi.org/10.1016/C2009-0-26589-5.
20. Frisch, M. J.; Trucks, G. W.; Schlegel, H. B.; Scuseria, G. E.; Robb, M. A.; Cheeseman, J. R.; Scalmani, G.; Barone, V.; Petersson, G. A.; Nakatsuji, H.; Li, X.; Caricato, M.; Marenich, A.; Bloino, J.; Janesko, B. G.; Gomperts, R.; Mennucci, B.; Hratchian, H. P.; Ortiz, J. V.; Izmaylov, A. F.; Sonnenberg, J. L.; Williams-Young, D.; Ding, F.; Lipparini, F.; Egidi, F.; Goings, J.; Peng, B.; Petrone, A.; Henderson, T.; Ranasinghe, D.; Zakrzewski, V. G.; Gao, J.; Rega, N.; Zheng, G.; Liang, W.; Hada, M.; Ehara, M.; Toyota, K.; Fukuda, R.; Hasegawa, J.; Ishida, M.; Nakajima, T.; Honda, Y.; Kitao, O.; Nakai, H.; Vreven, T.; Throssell, K.; Montgomery Jr., J. A.; Peralta, J. E.; Ogliaro, F.; Bearpark, M.; Heyd, J. J.; Brothers, E.; Kudin, K. N.; Staroverov, V. N.; Keith, T.; Kobayashi, R.; Normand, J.; Raghavachari, K.; Rendell, A.; Burant, J. C.; Iyengar, S. S.; Tomasi, J.; Cossi, M.; Millam, J. M.; Klene, M.; Adamo, C.; Cammi, R.; Ochterski, J. W.; Martin, R. L.; Morokuma, K.; Farkas, O.; Foresman, J. B.; Fox, D. J. Gaussian 09, Rev. D.01, Gaussian Inc., Wallingford, CT. (2009).
21. Becke, A. D. Density-functional thermochemistry. III. The role of exact exchange. *The Journal of Chemical Physics* **1993,** *98* (7), 5648–5652. https://doi.org/10.1063/1.464913.
22. Spychala, J. A Convenient Way to Methylated 2-Imidazolines. Syntheses of Fluorene and Triazine Cyclic Diamidines. *Monatsh Chem* **2006,** *137* (9), 1203–1210. https://doi.org/10.1007/s00706-006-0516-y.
23. Andreu, R.; Carrasquer, L.; Franco, S.; Garín, J.; Orduna, J.; Martínez de Baroja, N.; Alicante, R.; Villacampa, B.; Allain, M. 4H-Pyran-4-ylidenes: Strong Proaromatic Donors for Organic Nonlinear Optical Chromophores. *J. Org. Chem.* **2009,** *74* (17), 6647–6657. https://doi.org/10.1021/jo901142f.

Information about the authors:
Iryna V. Kurdiukova (*corresponding author*), Ph.D. in Chemistry, Senior Researcher of the Colour and Structure of Organic Compounds Department, Institute of Organic Chemistry of the National Academy of Sciences of Ukraine; https://orcid.org/0000-0001-6695-8535; e-mail for correspondence: *irina.kurdiukova@gmail.com.*
Volodymyr V. Kurdyukov, Ph.D. in Chemistry, Senior Researcher of the Colour and Structure of Organic Compounds Department, Institute of Organic Chemistry of the National Academy of Sciences of Ukraine; https://orcid.org/0000-0002-7668-5435.
Andrii V. Kulinich, Dr.Sci in Chemistry, Leading Researcher of the Colour and Structure of Organic Compounds Department, Institute of Organic Chemistry of the National Academy of Sciences of Ukraine; https://orcid.org/0000-0002-0857-6632.

ISSN 2308-8303 (Print) / 2518-1548 (Online)